Simulations of external multi-particle DLA on the plane and connections to the super-cooled Stefan problem

Alex Negrón[1] **and Sergey Nadtochiy**[1]

[1]Department of Applied Mathematics, Illinois Institute of Technology

We consider the external multi-particle diffusion-limited aggregation (MDLA) process on the 2-dimensional integer grid. In this random growth process, particles are distributed uniformly at random on the grid and undergo a simple symmetric random walk with exclusion. They walk until they contact a collection of particles centered at the origin, at which point they attach. Iterating this process, a cluster forms. Since its inception, DLA models in the plane have resisted rigorous mathematical treatment. Whereas mathematicians have succeeded in establishing scaling limits for other stochastic growth models, this result for DLA processes remains elusive. Recent findings in (1) establish a connection between the 1-dimensional MDLA process and solutions to a partial differential equation known as the super-cooled Stefan problem in one space dimension (1SSP). By fully characterizing the solutions to 1SSP, scaling limits for the 1-dimensional MDLA process were proven. It is natural to conjecture that a similar connection holds between 2-dimensional MDLA and SSP in two space dimensions. To address this conjecture, we take a numerical approach. We simulate the 2-dimensional MDLA process by decreasing the grid mesh towards 0. By studying the regularity of the cluster's interior and the statistical properties of its boundary, we show that the 2-dimensional MDLA process does not converge to solutions of 2SSP. We discuss why this process fails and propose possible resolutions.

Diffusion limited-aggregation | Super-cooled Stefan problem

Stochastic growth processes of the diffusion-limited aggregation (DLA) type have attracted great interest since their introduction by Witten and Sander in (11). In this classical DLA model, we start with a single seed point centered at the origin of $\mathbb{Z}^2$, and generate a second particle according to a chosen distribution away from the seed point, and allow this particle to take steps of unit size following a symmetric random walk. This particle walks until it visits a site adjacent to the seed, at which point the particle attaches to the cluster. A third particle is spawned on $\mathbb{Z}^2$ away from the cluster and follows a symmetric random walk until it contacts the cluster and attaches. We iterate this process until the cluster grows to some satisfactory size. Rosenstock and Marquardt expanded the original DLA model in (7) by letting the aggregate grow in $\mathbb{Z}^d$ by starting with the initial cluster as a point $\{0\}$, and attaching a neighboring site whenever a particle from a process evolving outside of the aggregate enters a site adjacent to the aggregate. Notably, in contrast to the classical DLA model, these particles evolve simultaneously. We refer to such a growth process as multi-particle DLA (MDLA). Much of the interest in DLA-type models focuses on the dendritic nature of the aggregates formed. These structures qualitatively agree with the shapes observed experimentally in crystallization, electrodeposition, and bacteria colony growth (8).

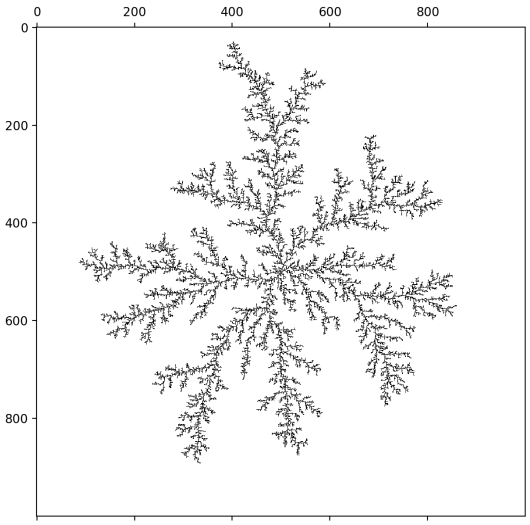

Fig. 1. Classical DLA cluster for $N = 1000$.

To illustrate the dendritic and fractal-like nature of the boundary of DLA aggregates, we have implemented a variant of the classical DLA model with several convenient optimizations made to reduce computational costs. Algorithm 1 is capable of producing a cluster on a 1000×1000 grid in four hours, running in Python.

Many numerical simulation studies of the aggregates resulting from DLA (6, 9, 10) have led to estimations of the fractal dimension of the aggregate as ≈ 1.7 in two space dimensions (4, 5). Despite the interest in DLA processes, the mathematical theory of such processes in $\mathbb{Z}^d$ for $d \geq 2$ is poorly understood. Indeed, Sander describes the DLA process as a "devilishly difficult model to solve, even approximately" in (11). For the aggregate in (9), the only rigorous mathematical results we have is an upper bound on its radius upon the attachment of n sites, and an almost sure convergence to infinity of the number of "holes" in the aggregate when $d = 2$ (3).

Connection to the super-cooled Stefan problem

In one space dimension $d = 1$ progress towards a mathematically rigorous understanding of DLA has been made. In (2), it is shown that the path of the right endpoint of the aggregate converges to the free boundary Λ in the *single-phase super-cooled Stefan problem* (1SSP) for the heat equation up to an

Algorithm 1: Classical DLA with optimization

Input: N, r, R
Initialize an $N \times N$ matrix A of zeros. Denote the entry at the center of this matrix $A_{\frac{N}{2},\frac{N}{2}}$.
For the seed particle, set $A_{\frac{N}{2},\frac{N}{2}} = 1$
while *cluster radius* $< R$ **do**
  Spawn a particle p uniformly at random on a circle of radius r centered at $(N/2, N/2)$.
  while *p is neither adjacent to a site in the cluster, adjacent to a site on the boundary of* Γ*, nor at a distance R from the seed* **do**
    Step p in a random direction: up/down/left/right with equal probability
    if *Distance between p to seed* $> R$ **then**
      Remove p and spawn a new one at radius r.
    else if *p is adjacent to a cluster site* **then**
      Set corresponding `matrix` entry to 1
      if *the distance from p to the seed is greater than r* **then**
        $r = r + 1$
  end
end
Print image of A, coloring all 1s black and all 0s white.

appropriate scaling of time. The classical 1SSP in one spatial dimension models the freezing of a supercooled liquid on the half-line strip $[0, \infty)$. The initial temperature of the liquid is lower than the temperature maintained at the liquid's surface, which lies below the freezing point of the liquid in question. The main result of (1) defines this problem as follows

$$\partial_t u = \frac{1}{2}\partial_{xx} u, \qquad \alpha\Lambda_t < x < \infty, \quad t \geq 0, \quad [1]$$

$$u(t, \alpha\Lambda_t) = 0, \qquad t \geq 0, \quad [2]$$

$$\partial_x u(t, \alpha\Lambda_t) = -2\alpha\dot{\Lambda}_t, \qquad t \geq 0, \quad [3]$$

$$u(0, x) = -\alpha f(x), \qquad x \geq 0.[\quad [4]$$

where $f \geq 0$ and $\alpha > 0$. We interpret t, x, and $u = u(t, x)$ as time, position, and temperature, respectively. The freezing point is captured by $u = 0$, and the "freezing front" (i.e., the interface between solid and liquid phases) at time t is located at position $x = \alpha\Lambda_t$. We assume $\alpha > 0$ is a given constant and f is a known probability density function. Equation [4] implies the liquid is below or at its freezing point, and hence why we call this the *supercooled* Stefan problem. Equation [1] models the heat diffusion in the fluid phase. Equation [2] states that the phase change at the front is isothermal. Equation [3] is the *Stefan condition*, which balances the heat flux through the freezing front with the exothermic heat release as the liquid freezes. This set of equations describes the *one-phase* problem, meaning that it assumes the temperature in the solid is constant and equal to $u = 0$. A solution to the SSP is the pair (u, Λ) such that Equations [1]-[4] are satisfied.

In this supercooled setting, despite living only in one dimension, the Stefan problem for the heat equation gives rise to singularities (in the sense that the velocity of the free boundary explodes in finite time). This corresponds to the "rapid freezing" of supercooled liquids observed experimentally. Still, for an appropriate notion of solutions for 1SSP (i.e., the "probabilistic solution"), global existence and uniqueness of such solutions have been recently shown in (1). The probabilistic reformulation of 1SSP corresponds to a 1-dimensional MDLA process described above.

Motivated by this connection between MDLA and 1SSP in one space dimension, we explore the possible connection between a suitable version of MDLA and 1SSP for the heat equation in two spatial dimensions. Our approach throughout is numerical. We simulate the two-dimensional MDLA process on integer grids with finer and finer mesh. We study whether the resulting clusters satisfy certain properties that (suitably defined probabilistic) solutions to 1SSP in two space dimensions ought to satisfy.

An MDLA process suitable for 1SSP in two spatial dimensions

We now consider an appropriate formulation of the MDLA process with connections to 1SSP. With this model defined, we will empirically confirm theoeretical predictions about the properties of this model's large population limit. To introduce this MDLA process, we consider the assumptions made by the classical DLA model that are inconsistent with the physics underlying 1SSP:

1. The seed is a *single infinitesimal particle.*
2. The cluster growth process terminates once the cluster attains some satisfactory size.
3. Particles are released, randomly walk, and are attached *one at a time.*
4. Particles are "removed" when they drift too far from the cluster.

To amend these assumptions and formulate an algorithm modeling solutions to 1SSP in two space dimensions, we introduce the new set up as follows.

Denote the set of points belonging to the cluster as Λ_t^N on the $N \times N$ grid Γ^N, and denote the seed Λ_0. To store this data, we use an $N \times N$ matrix A to represent Γ^N. Any point $(x, y) \in \Gamma^N$ corresponds to the entry at row y, column x in A. Entries $A_{y,x}$ corresponding to sites (x, y) which belong to the cluster Λ_t^N are filled with a value of 1, and all other entries a value of 0.

In the classical setting, Λ_0 is the singleton set consisting of one seed particle of negligible volume. In the Stefan setting, Λ_0 has a strictly positive volume and therefore consists of more than one particle. If Λ_0 contains P particles, then we say $P = kN^2$ for some $k \in (0, 1)$. To see how the shape of Λ_0 influences the terminal shape of Λ_t^N, we study three different types of Λ_0 seed clusters: circle, square, and cross. Note that for a circular seed cluster, the radius r of a circular seed is given by

$$r^2 = \frac{kN^2}{\pi}.$$

Instead of releasing particles and walking them one-by-one, we now release M particles on Γ^N/Λ_0 at time $t = 0$ all at once. For each site $(x, y) \in \Gamma^N \setminus \Lambda_0$, we place a particle at (x, y) with probability p. Each particle follows a symmetric nearest-neighbor random walk as they do in classical DLA, but here we enforce two additional properties on this random

walk. Firstly, we require the particles to follow a random walk with *exclusion*, by which we mean no two particles are permitted to occupy the same site at the same time. If a particle attempts to step into an occupied site, it stays put. Secondly, we require particles to follow a random walk with *reflection* at the boundary of Γ^N : if a particle attempts to step outside Γ^N, it stays put. The cluster growth process terminates at time $t = TN^2$ or when all of the M particles released at $t = 0$ have attached to Λ_t^N, whichever occurs first.

In the next section we numerically study the properties of the terminal cluster $\Lambda_{N^2T}^N$ as $N \to \infty$. To implement the model for increasing N, we fix integers $N_0 > 0$ and $N^* > N_0$. We run the model for each integer $N \in [N_0, N^*]$. This algorithm is shown in Algorithm 2.

Algorithm 2: Modified DLA, circular seed cluster.

Input: N_0, N^*, T, $p \in (0,1)$, $k \in (0,1)$
for $N \in [N_0, N^*]$ **do**
  Initialize an $N \times N$ matrix A of zeros.
  For all entries $A_{i,j}$ of matrix A, if the Euclidean distance between (j,i) and $(N/2, N/2)$ is less than kN^2/π, set $A_{i,j} = 1$.
  Let B denote the set of all the sites (j,i) for which $A_{i,j} = 0$ (this is the set $\Gamma^N \setminus \Lambda_0$.) For each $(j,i) \in B$, with probability p set $A_{i,j} = 2$. Let P be the set of all such sites. Denote $M = |P|$.
  Set $t = 0, m = 0$.
  while $t < TN^2$ *and* $m < M$ **do**
    for $p = (x,y) \in P$ **do**
      p takes a step to $p^* = (x^*, y^*)$ according to the nearest-neighbor symmetric reflected random walk with exclusion. If this p^* is unoccupied, p steps to p^*.
      if p^* *is adjacent to a site in* Λ_t^N **then**
        Observe that it is possible for particles to be in positions adjacent to p^* at the time of attachment. Denote $\tilde{P}^*$ the collection of particles connected to p^*. Once p^* is attached to Λ_t^N, all the particles in $\tilde{P}^*$ must also be attached since they are instantaneously connected to Λ_t^N.
        To attach all of the particles connected to p^*, we use the `flood-fill` algorithm to identify which positions are connected to p^* and store them in $\tilde{P}^*$.
        for $\tilde{p} = (\tilde{x}, \tilde{y}) \in \tilde{P}^* \cup \{p^*\}$ **do**
          Attach $\tilde{p}$ to Λ_t^N by setting $A_{\tilde{y},\tilde{x}} = 1$ and $A_{y,x} = 0$.
        end
        $m = m + 1$
    end
    $t = t + 1$
  end
end

Each of the terminal clusters showed in Figure 2 were produced using Algorithm 2 for various seed shapes. These clusters were formed for $k = 0.01, T = 0.01$, and $p = 0.25$. We see that for each initial seed shape, the shape of the terminal clusters $\Lambda_{N^2T}^N$ is similar: fractal-like "branches" form on the seed. This

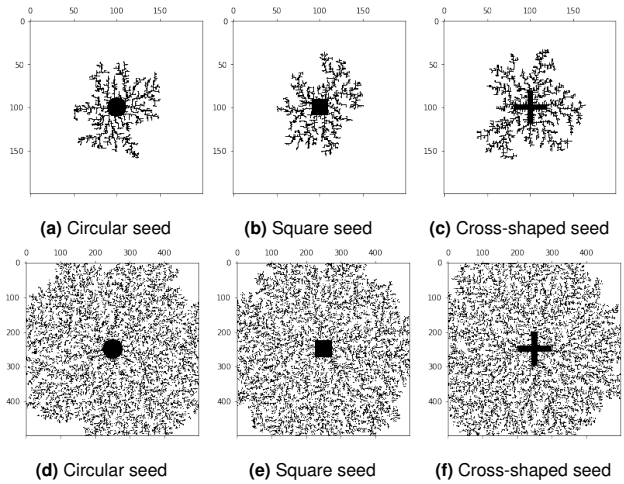

(a) Circular seed **(b)** Square seed **(c)** Cross-shaped seed

(d) Circular seed **(e)** Square seed **(f)** Cross-shaped seed

Fig. 2. Terminal clusters at $N = 200$ (top row) and $N = 500$ (bottom row).

type of cluster is what we would expect for the classical DLA model with a positive-volume seed. Note as well that there does not appear to be any obvious difference in the shape of $\Lambda_{N^2T}^N$ for different shapes of Λ_0. In particular, Figure 2f implies that the qualitative structure of the terminal clusters $\Lambda_{N^2T}^N$ does not depend on the convexity of the seed Λ_0.

$\Lambda_{N^2T}^N$ as $N \to \infty$: random or deterministic limit?

In the previous section we saw an indication that the shape of the terminal cluster $\Lambda_{N^2T}^N$ is invariant with respect to the shape of the seed Λ_0 (see Figure 2). In this section, we test whether the limit $\Lambda_T = \lim_{N\to\infty} \Lambda_{N^2T}^N$ is random or deterministic. The result in (1) proves the existence of this limit in the weak sense, but it is unclear whether this limit is random or deterministic. Ongoing research predicts the limit is random. To test this hypothesis numerically, we perform the following experiment.

Fix a number S of Monte Carlo simulations and fix two reference points

$$x_c, x_s \in \Gamma^N \setminus \Lambda_0.$$

Reference point x_c is positioned near the corner of Γ^N at coordinate $(.95N, .95N)$, and reference point x_s is positioned towards the side of of Γ^N at coordinate $(.95N, .50N)$. Let $d(\cdot,\cdot)$ be the L^1 distance function. Fix a step size z. We run the cluster growth simulation S times and for each $N = N_0, N_0 + z, N_0 + 2z, \ldots$ we plot the histogram of the distances from x_s and x_c to $\Lambda_{N^2T}^N$. Since the length of a cell's edge on Γ^N is $1/N$, the "physical" distance from $x = x_c, x_s$ to $\Lambda_{N^2T}^N$ is calculated as

$$d(x, \Lambda_{N^2T}^N) = \frac{1}{N} \inf_{p \in \Lambda_{N^2T}^N} d(x,p).$$

Similarly, for each N and for each sensor we also plot the distance sample mean

$$\hat{\mu}_d = \frac{1}{S} \sum_{i=1}^{S} d(x, \Lambda_{N^2T}^N),$$

and sample variance

$$\hat{\sigma}_d^2 = \frac{1}{S-1} \sum_{i=1}^{S} \left(d(x, \Lambda_{N^2T}^N) - \hat{\mu}_d \right)^2$$

as functions of N.

If $\hat{\sigma}_d^2$ appears to converge to 0 for both sensors, or equivalently if the histograms appear to converge to a Dirac mass, then we can conclude that the limit of $\Lambda^N_{N^2T}$ is deterministic. Otherwise the limit is random.

Experiment results for a circular seed cluster. Our experiment uses $S = 10$ simulations and N ranges from $N_0 = 100$ through $N^* = 500$ with a step size of $z = 10$. We set $k = 0.01, T = 0.01$, and $p = 0.25$. Figure 3 shows the results of the experiment for the sensor x_s and Figure 4 shows the results for sensor x_c.

For both sensors, the histograms of the distance samples do not suggest convergence to a Dirac mass. Whereas the variance plot for sensor x_s appears to converge to 0 as N increases, the variance plot for sensor x_c does not appear to converge to zero. Therefore the results of this experiment indicate that the limit of $\Lambda^N_{N^2T}$ as $N \to \infty$ is random.

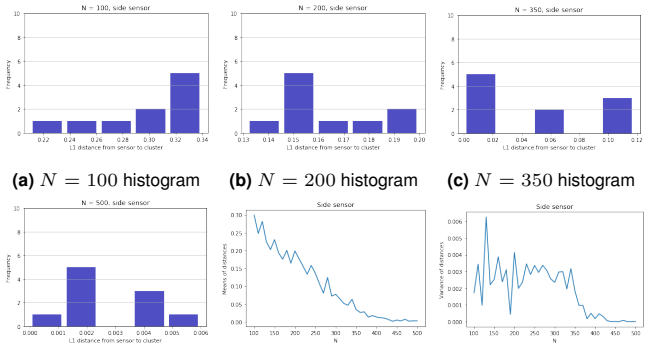

(a) $N = 100$ histogram **(b)** $N = 200$ histogram **(c)** $N = 350$ histogram

(d) $N = 500$ histogram **(e)** Sample means **(f)** Sample variances

Fig. 3. Side sensor x_s: distance histograms, sample mean and variance plots.

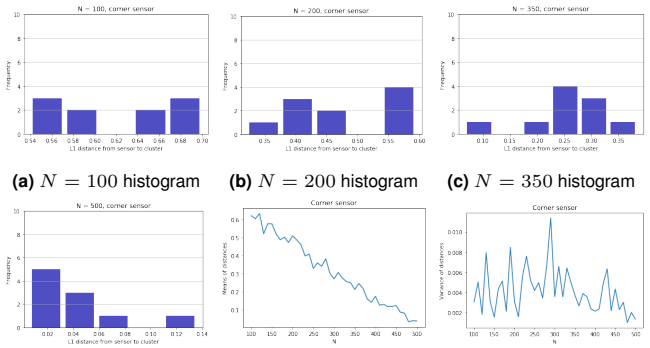

(a) $N = 100$ histogram **(b)** $N = 200$ histogram **(c)** $N = 350$ histogram

(d) $N = 500$ histogram **(e)** Sample means **(f)** Sample variances

Fig. 4. Corner sensor x_c: distance histograms, sample mean and variance plots.

The difference of the results for each sensor deserves attention. The sample mean plots show that the distance from x_s to the cluster goes to zero much quicker than it does for x_c. This is evidenced in Figure 2. In the bottom row, the images indicate that the cluster spreads to the side of the grid before it spreads into the corner. There is a sense in which it is "more difficult" for the cluster to grow into the corner of the grid than it is for the cluster to grow to the side.

Properties of $\Lambda_T = \lim_{N\to\infty} \Lambda^N_{N^2T}$

If $\Lambda_T = \lim_{N\to\infty} \Lambda^N_{N^2T}$ is a classical solution to the super-cooled Stefan problem in two dimensions, there are certain properties we expect Λ_T to have. These properties are outlined below:

a.) Since particles aggregate to the cluster randomly, situations may occur when a small "hole" is created in the cluster and is never filled with a particle. For Λ_T to solve the super-cooled Stefan problem in dimension two in the classical sense, the total limiting volume of these holes should be negligible. In dimension one, such holes are impossible. However, new results indicate that in dimension two, the total limiting volume of these holes may not be negligible.

b.) The length of the boundary of $\Lambda^N_{N^2T}$ does not explode as $N \to \infty$. Likewise, the volume of the cells comprising this boundary does not explode.

In the consideration of this boundary, we introduce two different notions of the boundary. Denote with $\partial\Lambda^N_{N^2T}$ the usual topological boundary. We also consider $\overline{\partial}\Lambda^N_{N^2T}$, the "external" boundary of $\Lambda^N_{N^2T}$. The external boundary is defined as

$$\overline{\partial}\Lambda^N_{N^2T} = \partial\Lambda^N_{N^2T} \setminus \partial H^N_{N^2T},$$

where $H^N_{N^2T}$ is the set of holes in the cluster $\Lambda^N_{N^2T}$. For example, the external boundary is the boundary of the cluster in Figure 4 excluding the ten edges lining the holes.

c.) Since the boundary of the grid Γ^N and the seed Λ_0 are symmetric, we expect the limiting cluster Λ_T to also be symmetric.

In this section we numerically test each of these properties to determine whether Λ_T forms a solution to the super-cooled Stefan problem.

We can test (a) and (b) together with the same procedure, stemming from a simple observation. The following figure represents the matrix A from Algorithm 2 where the 1s indicate particles belonging to $\Lambda^N_{N^2T}$, and blank spaces are 0s.

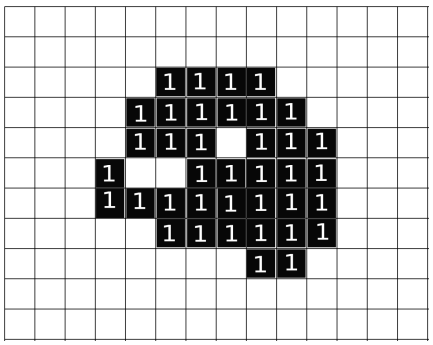

Fig. 5. Example of a cluster with holes of different size.

Note that $\partial\Lambda^N_{N^2T}$ is comprised of the edges on the exterior of the cluster and the edges lining the interior holes. To compute the length of this boundary, we must count the number of these edges. Let E^N denote the value of this count. Let E_{ij} be

the of edges of the cell associated to entry A_{ij} which contribute to $\partial\Lambda^N_{N^2T}$. We can compute E_{ij} using

$$E_{ij} = 4 - \sum(\text{adjacent entries}),$$

where the adjacent entries are the entries representing cells above, below, to the right, and to the left. For example, consider the bottom-right-most cluster cell. This cell has neighbors of value 1 above and to the left, and neighbors of value 0 below and to the right. Thus it contributes $E_{ij} = 2$ edges to $\partial\Lambda^N_{N^2T}$, verified by the picture. It is clear that

$$|\partial\Lambda^N_{N^2T}| = E^N = \sum_{i,j} E_{ij}.$$

Note that $|\overline{\partial}\Lambda^N_{N^2T}| \leq |\partial\Lambda^N_{N^2T}|$, where equality holds when there are no holes in $\Lambda^N_{N^2T}$ and the inequality is strict when there are holes. To count the edges that contribute only to $\overline{\partial}\Lambda^N_{N^2T}$, we need to modify the procedure above.

We begin by "filling" all the holes with a well-chosen value. Everywhere in matrix A where entries correspond to holes in $\Lambda^N_{N^2T}$, we fill these entries with -1. Then for each entry A_{ij}, we compute E_{ij} similarly as above, but here we take the absolute value of each adjacent entry:

$$\overline{E}_{ij} = 4 - \sum |\text{adjacent entries}|$$

so that

$$|\overline{\partial}\Lambda^N_{N^2T}| = \overline{E}^N = \sum_{i,j} \overline{E}_{ij}.$$

The normalized values $L^N_{\partial\Lambda} = E^N/N$ and $\overline{L}^N_{\partial\Lambda} = \overline{E}^N/N$ give the lengths of the boundary and external boundary, respectively.

To fill the holes, we utilize the so-called "flood-fill" algorithm. The flood-fill algorithm is used to determine the area connected to a given node in a multi-dimensional array. An example of its application is the "bucket" fill tool in digital painting programs used to fill connected areas of a similar coloring with a different color. In our setting, the flood fill algorithm fills connected areas in matrix A which have similar values. We choose entry $A_{0,0} = 0$ as the initial input to the flood-fill algorithm. The algorithm changes this value to $A_{0,0} = -1$. It then checks the values of neighboring entries $A_{1,0}$ and $A_{0,1}$. If these entries are equal to 0, it changes them to -1. The process repeats for each $A_{1,0}$ and $A_{0,1}$ and so on until the entire area of entries connected to $A_{0,0}$ initially having value 0, now have value -1.

To illustrate the application of flood-fill, observe that one application of flood-fill to Figure 4 changes all cells with value 0 exterior to the cluster to -1. Then, we set all remaining entries of A with value 0 to -1. These entries of value 0 that were not changed by flood-fill are the holes themselves, as they are not connected to $A_{0,0}$. Now that all the holes have value -1, what remains is to change the values of -1 exterior to the cluster back to 0. To do this, we apply flood-fill again to entry $A_{0,0} = -1$, this time specifying that the algorithm change all values of -1 to 0. The result is a matrix A^* whose entries representing holes in the cluster $\Lambda^N_{N^2T}$ have been filled with -1.

We also want to compute the volume of cells on $\partial\Lambda^N_{N^2T}$. To do this, we need a count of how many cells live on the boundary $\partial\Lambda^N_{N^2T}$, and then we make an appropriate normalization for the physical volume. For each entry A_{ij} in matrix A, we check the following conditions. If at least one of them holds then entry A_{ij} lives on the boundary of $\Lambda^N_{N^2T}$:

1. $A_{i+1,j} = 1$ and $A_{i-1,j} = 0$,
2. $A_{i-1,j} = 1$ and $A_{i+1,j} = 0$,
3. $A_{i,j+1} = 1$ and $A_{i,j-1} = 0$,
4. $A_{i,j-1} = 1$ and $A_{i,j+1} = 0$.

The first condition says that the position below A_{ij} is a cluster particle and the position above A_{ij} is an empty cell, the second condition is the converse, and the third and fourth conditions are analogous but for positions left and right of A_{ij}. It is is clear that if any one of these hold, A_{ij} must be on the boundary of $\Lambda^N_{N^2T}$. To compute the physical volume of these boundary cells, if B^N denotes the number of cells on the boundary $\partial\Lambda^N_{N^2T}$ then the volume of the boundary is

$$V^N_{\partial\Lambda} = \frac{1}{N^2} B^N.$$

In the course of filling holes, we may also keep count of how many holes are filled. In this way, we determine the number of holes H^N in $\Lambda^N_{N^2T}$. To compute the physical volume of these holes, we take

$$V^N_{\text{holes}} = \frac{1}{N^2} H^N.$$

To test for the symmetry of Λ_T, for each N we take the 90 degree counterclockwise rotation of $\Lambda^N_{N^2T}$, then compute the volume of the particles in the symmetric difference between $\Lambda^N_{N^2T}$ and its rotated counterpart. If this volume converges to 0 as a function of N, we conclude that Λ_T is symmetric. More explicitly, denote $\text{rot}(\Lambda^N_{N^2T})$ the $+90$ degree rotation of $\Lambda^N_{N^2T}$. For each N, count the number of particles in the symmetric difference

$$D^N = |\Lambda^N_{N^2T} \triangle \text{rot}(\Lambda^N_{N^2T})|,$$

so that the volume of the particles in this symmetric difference is given by

$$V^N_{\text{diff}} = \frac{1}{N^2} D^N.$$

Testing (a), (b), and (c) amounts to plotting $L^N_{\partial\Lambda}, \overline{L}^N_{\partial\Lambda}, V^N_{\partial\Lambda}$, V^N_{holes}, and V^N_{diff} as functions of N. The results of these tests with the same parameters as the experiment in Section 3.1 are shown in Figure 6. Figure 6-(a) and (b) demonstrate that the length of the boundary of Λ_T explodes as a function of N. Figure 6-(d) indicates that the holes constitute a non-negligible volume in the limiting cluster Λ_T. The spiking of the graphs in (b) and (d) is due to how particles are attached in Algorithm 2. When a particle enters a position adjacent to the cluster, if there are particles connected to this adjacent site, then all the particles attach instantly. This result in large "pockets" of holes forming in the cluster, producing sharp up-spikes in hole volume and a corresponding down-spikes in the external boundary length. Nevertheless, it is clear that the experiment confirms theoretical conclusions that the holes in the two dimensional cluster growth process constitute a non-negligible volume. Likewise, Figure 5-(e) suggests the volume of particles in $\Lambda^N_{N^2T} \triangle \text{rot}(\Lambda^N_{N^2T})$ is strictly positive as $N \to \infty$. This means that the symmetry of the seed cluster Λ_0 is not preserved in the cluster growth process as N increases. In particular,

these results imply that *the MDLA model considered here does not converge to solutions of 1SSP in two space dimensions.*

Note that Figure 6 also includes a plot of first exit times. These are the times $t \in [0, TN^2]$ for which the cluster first contacts the boundary of Γ^N. The decreasing trend of these exit times suggests that the cluster fills Γ^N instantaneously in the limit as $N \to \infty$.

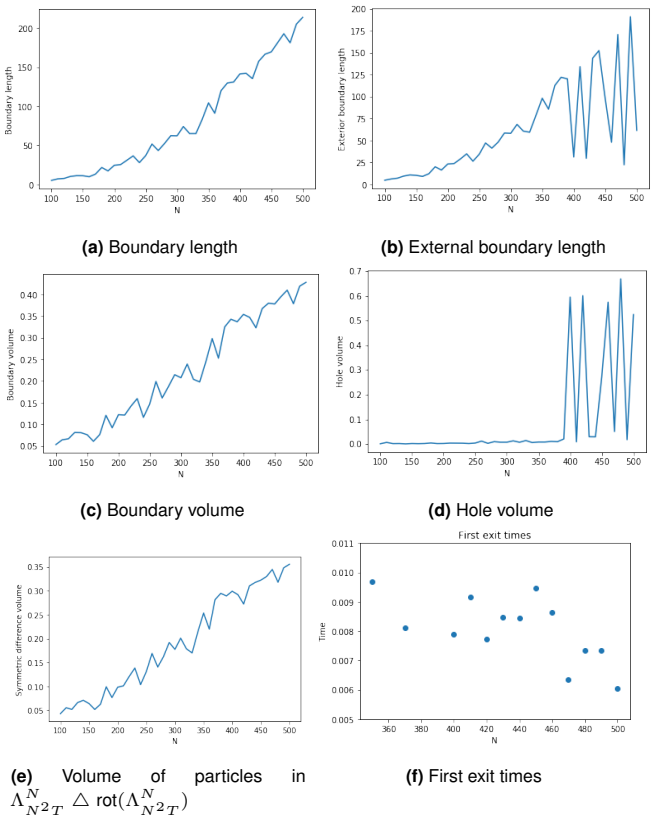

(a) Boundary length **(b)** External boundary length

(c) Boundary volume **(d)** Hole volume

(e) Volume of particles in $\Lambda^N_{N^2T} \triangle \text{rot}(\Lambda^N_{N^2T})$ **(f)** First exit times

Fig. 6. Test results for properties (a), (b), and (c).

Conclusion

Our statistical analysis of 2-dimensional MDLA terminal aggregates shows that the MDLA process defined herein does not converge to probabilistic solutions of 1SSP in two space dimensions. In particular, the presence of a non-negligible hole volume in terminal aggregates grown on grids with a fine mesh and that these terminal aggregates do not appear to converge to deterministic structures disqualify $\lim_{N\to\infty} \Lambda^N_{N^2T}$ as a probabilistic solution to 1SSP in two space dimensions. An unexpected consequence of this work is an observation obtained from Figure 6(f). This plot indicates that the terminal cluster first exit times go to 0 as $N \to \infty$. In other words, we conjecture that terminal clusters spread to the boundary of Γ^N instantaneously in the limit as $N \to \infty$.

Although MDLA clusters do not appear to converge to solutions of 1SSP in two space dimensions, it is possible that modifications may be made to the MDLA process studied here such that the terminal clusters do not have the numerous undesirable properties identified in our simulations. In particular, if it is possible to introduce a feature to the MDLA process that results in a more regular and less fractal-like terminal cluster boundary, and if it is possible to limit the possibility of interior hole formation, such a process may produce limiting clusters that do indeed converge to solutions.

References

1. F. Delarue, S. Nadtochiy, and M. Shkolnikov, *Global solutions to the supercooled stefan problem with blow-ups: regularity and uniqueness*, arXiv preprint arXiv:1902.05174, (2019).
2. A. Dembo and L.-C. Tsai, *Criticality of a randomly-driven front*, Archive for Rational Mechanics and Analysis, 233 (2019), pp. 643–699.
3. D. M. Eberz-Wagner, *Discrete growth models*, arXiv preprint math/9908030, (1999).
4. M. B. Hastings and L. S. Levitov, *Laplacian growth as one-dimensional turbulence*, Physica D: Nonlinear Phenomena, 116 (1998), pp. 244–252.
5. P. Meakin, *Formation of fractal clusters and networks by irreversible diffusion-limited aggregation*, Physical Review Letters, 51 (1983), p. 1119.
6. ———, *Multiparticle diffusion-limited aggregation with strip geometry*, Physica A: Statistical Mechanics and its Applications, 153 (1988), pp. 1–19.
7. H. B. Rosenstock and C. L. Marquardt, *Cluster formation in two-dimensional random walks: application to photolysis of silver halides*, Physical Review B, 22 (1980), p. 5797.
8. L. M. Sander, *Diffusion-limited aggregation: a kinetic critical phenomenon?*, Contemporary Physics, 41 (2000), pp. 203–218.
9. R. F. Voss, *Multiparticle diffusive fractal aggregation*, Physical Review B, 30 (1984), p. 334.
10. ———, *Multiparticle fractal aggregation*, Journal of Statistical Physics, 36 (1984), pp. 861–872.
11. T. Witten Jr and L. M. Sander, *Diffusion-limited aggregation, a kinetic critical phenomenon*, Physical review letters, 47 (1981), p. 1400.